Springer

Journal of Mechanical Science and Technology 23 (2009) 3416~3423

Journal of Mechanical Science and Technology

www.springerlink.com/content/1738-494x
DOI 10.1007/s12206-009-1016-x

A numerical study on the flow and heat transfer characteristics in a non-contact glass transportation unit †

Ik-Tae Im[1,*], Chan Woo Park[1] and Kwang Sun Kim[2]

[1]*Department of Mechanical Design Engineering, College of Engineering, Chonbuk National University, 664-14, Duckjin-dong 1-ga, Duckjin-gu, Jeonju, 561-756, Korea*
[2]*Department of Mechatronics Engineering, Korea University of Technology and Education, 307 Gajeonri, Byungchon-myeon, Chonan, 330-860, Korea*

(Manuscript Received February 17, 2009; Revised July 28, 2009; Accepted August 10, 2009)

Abstract

Vertical sputtering systems are key equipment in the manufacture of liquid crystal display (LCD) panels. During the sputtering process for LCD panels, a glass plate is transported between chambers for various processes, such as deposition of chemicals on the surface. The minimization of surface scratches and damage to the glass, the rate of consumption of gas, and the stability of the floating glass-plate are key considerations in the design of a gas pad. To develop new, non-contact systems of transportation for large, thin glass plates, various shapes of the nozzle of a gas pad unit were considered in this study. In the proposed nozzle design, negative pressure was used to suppress undesirable fluctuations of the glass plate. After the nozzle's shape was varied through numerical simulations in two dimensions, we determined the optimal shape, after which three-dimensional analyses were carried out to verify the results from the two-dimensional analyses. The rate of heat transfer from the glass plate, as a result of the gas jet, was also investigated. The average Nusselt number at the glass surface varied from 22.7 to 26.6 depending on the turbulence model, while the value from the correlation for the jet array was 23.5. It was found that the well-established correlation equation of the Nusselt number for the circular jet array can be applied to the cooling of the glass plates.

Keywords: Liquid crysral display panel; Non-contact transportation; Sputtering equipment; Computational fluid dynamics; Air cushion

1. Introduction

Liquid crystal displays (LCDs) are flat panel displays most widely used in various applications ranging from small cellular phones to large-sized television sets. A sputtering system, which is used to make gates, sources, electrodes of drain, common electrodes, indium tin oxide(ITO) pixels, and black matrix for color filters, is a key system in developing facilities during the manufacture of LCD. Due to the expanded sizes of products, such as personal computer (PC) monitors and television sets using LCDs, industries have focused on the use of large-sized glass plates to increase throughput and lower cost. Generation 7 (G7) production lines that use roughly 2,000 mm × 2,200 mm glass plates are currently in use. Meanwhile, G8 (or newer) production lines that will use wider glass plates than the G7 will eventually dominate the market.

A glass transportation unit picks up a glass plate and introduces it into a sputtering system. It then sequentially moves the plate to the loading chamber, buffer chamber, and process chamber for chemical deposition on the glass surface. In older, cluster-type sputtering systems, glass plates are moved horizontally, which necessitates a very large site in factories.

† This paper was recommended for publication in revised form by Associate Editor Jae Dong Chung
*Corresponding author. Tel.: +82 63 270 4761, Fax.: +82 63 270 4761
E-mail address: itim@jbnu.ac.kr

A vertical, stationary type of system, in which glass plates are moved in an almost vertical trajectory, is now adopted as a solution to overcome space restriction. However, mechanical friction, such as in between rollers and rails in transportation units, can create very tiny particles of dust that result in poor panel quality. Therefore, interests have grown in terms of developing non-contact techniques for transportation.

Several methods, including gas jets [1, 2], electrostatic force [1], and acoustic levitation [3], were reported as non-contact transportation techniques. The use of gas jets has little effect on the glass surface or the chemical process, whereas electrostatic force may influence it. It is difficult to use acoustic levitation for very large glass plates because of the low range of levitation.

In the past, we reported the shape of the gas pad for the levitation of glass in terms of the type of nozzle and the arrangement of nozzles and slots for effusion [2, 4, 5].The distances between nozzles or pitches along both horizontal and vertical directions were determined for minimizing gas consumption. The size of the effusion slots was determined to obtain an evenly-distributed pressure profile on the glass surface to avoid damaging the plate. On the basis of the analysis, the G7 glass plate was successfully levitated and moved using the gas pad.

One major concern for non-contact transportation techniques is stability during transportation. In contact-based methods of glass transportation that use chucks or carriers, processes instantaneously pause should there be a problem in the transportation unit. In non-contact transportation, an unstable, external disturbance can cause abrupt change or vibrations during levitation, which may cause the glass plate to break. If this occurs, the operation is completely stopped since the debris needs to be cleaned, but this takes time because the operation requires the system pressure to equal with the atmospheric pressure before the equipment is opened up. Thus, the throughput is lowered due to the shutdown of the system, and additional time and cost are needed to restore high state of vacuum into the system. Therefore, it is very important to prevent an unstable, external disturbance.

Gas pads, which were reported in the study and determined by numerical simulations of Jun et al. [5], could levitate and transport actual-sized glass plates. However, when gas pads are used, the glass plate vibrates during the initial stage of the transportation. Thus, the design of the gas-injection nozzle was considered in this study to prevent vibration. To improve the stability of the glass plates, the different shapes of the injection nozzle and the effusion holes were matched to generate a negative pressure distribution on the glass surface. The pressure distribution on the glass surface was first analyzed for various shapes of the gas pad prior the set-up of the experimental apparatus that would use the glass-plates.

During the manufacturing process, the glass plate is heated up to about 420 K in the heating chamber before its transfer to the process chamber where it will be coated by the sputtering process. If the temperature drops considerably, owing to the injected gas used to move the glass plate, during transport from heating chamber to process chamber, additional energy is required to heat up the glass plate. Therefore, the heat transfer characteristics of the glass surface that is impinged by a gas jet were also analyzed to check the drop in temperature during transportation.

2. Gas pad for the transportation of glass

Im et al. [2, 4, 5] studied the optimal design of the gas pad configuration that reduces gas consumption and pressure concentration on the glass surface. Two types of pad have been proposed for the G7 system. The first pad [2, 4] is composed of several lines of injection holes and effusion slots between the lines of the injection holes that regulate the pressure in the spaces between the glass plate and the gas pad. The second pad [5] is designed to lower gas consumption in comparison with the first pad. Injection and effusion holes are concentric rings wherein the inner circle is used for injection and outer ring is used for effusion.

Experiments on the use of the proposed nozzle-shape revealed successful levitation and transportation, but there vibrations were observed at the early stage. In this study, the shapes of the injection nozzle and the effusion holes were varied to minimize vibration. Fig. 1 shows a schematic of the nozzle part of the gas pad with a typical pressure-profile on the glass surface. A ring-type injection nozzle was designed in the shape of a bell; this ensures the presence of high pressure over a wide area surface. Following impinging, the flow of gas was accelerated through a narrow passage and lowered the pressure to negative values. This negative pressure acts like a chuck on the glass surface; hence, it is expected that stable conditions of

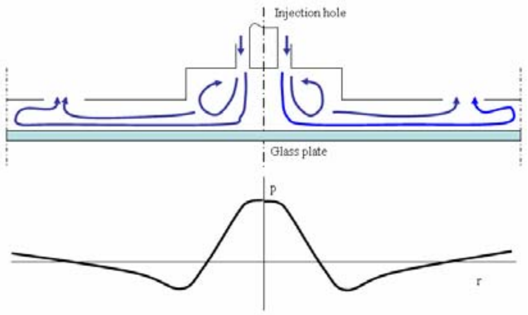

Fig. 1. Schematic diagram of a nozzle in a gas pad with a typical pressure distribution on the glass surface.

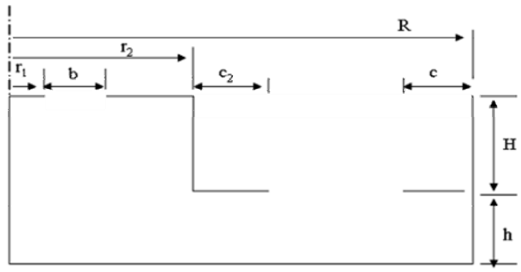

Fig. 2. Geometry of a gas pad for the analysis.

operation will be easily achieved compared to the previous design [5].

In consideration of geometrical symmetry, domain of analysis was chosen for this study, as illustrated in Fig. 2. The effects of the design variables on pressure distribution were numerically tested to obtain data for the design of the pad. Design variables include r_2 that confines the recirculation zone, the levitation height h, and variables c and c_2, which are related to the sizes and positions of the effusion holes. Prior to the analysis of the variation of the nozzle-shape, the base geometric dimensions were determined from previous studies [2, 4, 5]. Base geometry was used to test the grid system and turbulence-model conditions. The distance between the injection holes ($2R$) was set to 60 mm although the optimal value in previous studies were found to be dependent on r_2. Other dimensions were normalized by H as follows: $r_1/H = 0.33$, $r_2/H = 2.5$, $b/H = 0.5$, and $h/H = 0.83$. Variables related to the effusion holes, c and c_2, were both set to zero; that is, the holes are open to the surrounding in the base model.

3. Analysis

Assuming that the flow is incompressible and in a steady state with constant properties, the governing equations for the geometries shown in Fig. 2 were derivd as two-dimensional axisymmetric continuity and the well-known Reynolds-averaged Navier-Stokes equations with appropriate turbulence-model equations.

$$\frac{\partial U_i}{\partial x_i} = 0 \tag{1}$$

$$\rho U_j \frac{\partial U_i}{\partial x_j} = -\frac{\partial P}{\partial x_i} + \frac{\partial}{\partial x_j}\left(2\mu S_{ij} + \tau_{ij}\right) \tag{2}$$

where S_{ij} is the averaged strain-rate tensor that is given by

$$S_{ij} = \frac{1}{2}\left(\frac{\partial U_i}{\partial x_j} + \frac{\partial U_j}{\partial x_i}\right) \tag{3}$$

and τ_{ij} is the Reynolds-stress tensor,

$$\tau_{ij} = -\rho\overline{u_i' u_j'} \tag{4}$$

The incompressible flow assumption was developed based on the magnitude of gas velocity at the inlet. It was expected that a maximum value, about15 m/s, would cause no significant pressure build-up since the flow field was open to atmospheric conditions. Variations of the fluid properties according to temperature can also be neglected in the temperature range from 300 K to 420 K because they do not vary significantly. Instead, the properties at the film temperature were used for heat transfer calculations.

A constant inlet-velocity and temperature were imposed for the injection hole. The inlet-velocity was calculated from the assumption that the area integration of the pressure on the glass surface is equal to the weight of the glass plate. The gas temperature at the inlet was assumed to be 300K. A no-slip condition was applied to all the solid surfaces, such as the glass plate and the steel pad. A zero heat-flux condition was applied to the nozzle-wall for the sake of simplicity, and also because the wall was relatively thick, which implies that thermal conditions would remain similar across the entire wall of the nozzle.

The commercial computational fluid dynamics software, FLUENT [6], was used to solve the governing equations. The grid system was determined from the numerical experiments. Fig. 3 shows the results from the grid test. The pressure distribution did not

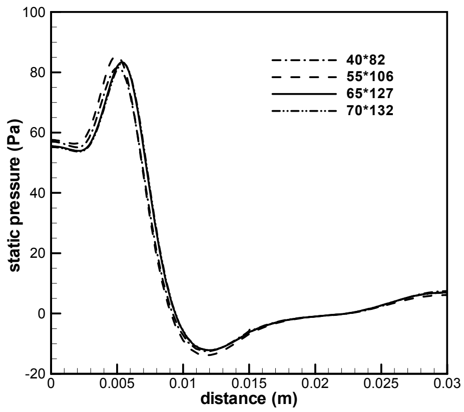

Fig. 3. Variation of the static pressure along the glass surface for the grid test.

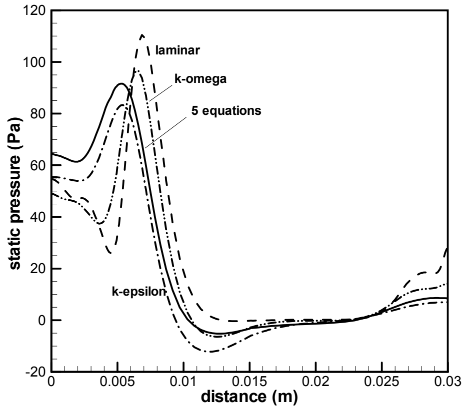

Fig. 4. Results from the turbulence model (the solid line depicted as '5-equations' are from the Reynolds Stress Model).

change in grids that are finer than 65×127; hence, this system was used throughout the flow calculations, although the location of the dense grid was changed according to the shape of the nozzle. The Nusselt number was investigated to find out the effects of the grid system on the heat transfer characteristics. The average Nusselt numbers for the same grid systems, as shown in Fig. 3, are 32.6, 35.0, 36.9, and 37.7, respectively. The Nusselt numbers along the glass surface for the 65×127 and 70×132 cases were almost duplicate profiles except for the vicinity at maximum point. The average value of the latter only slightly increased due to the increase in peak value. Therefore, the same grid systems (flow calculations) were used for the heat transfer calculations.

The flow was assumed to be turbulent because the Reynolds numbers based on h and ($h+H$), considering the properties of air at room temperature, are 5340 and 11750, respectively. The flow that was considered in this study is similar to the impinging jet at the early stage, which then transforms as a channel-flow between circular plates. Several turbulence-models were tested to find the proper turbulence-model for this flow situation. Fig. 4 shows the test results from the standard k-ε model [7], the k-ω model [8], and the Reynolds stress model [9], along with the results from the laminar flow for the sake of comparison. The result from the k-ω model is qualitatively similar to that of the laminar flow. The k-ε model and the Reynolds Stress Model yield similar profiles. The k-ε model was chosen because (i) it is cost-effective in the number of equations when compared to the RSM model; (ii) previous studies on turbulent coaxial confined the jet flow [10], showing the k-ε model to be successful in predicting the velocity profile along the radial direction; and (iii) the pressure distribution profile, rather than the quantitative value of the pressure, was deemed important in the design of the nozzle-shape because of the stability of a glass plate. The overall pressure for the lift can be adjusted up to certain range using the gas inlet velocity once the shape of the pad is determined.

4. Results and discussion

4.1 Shape of the injection nozzle

To determine the optimal shape of the nozzle, the first r_2 is changed. The recirculation zone, which is mainly due to the abrupt change in the direction of flow following impinging of the flow on the glass plate, freely develops as r_2 is increased. Fig. 5 shows the variation of the pressure coefficient c_p as r_2/H varies from 1.0 to 3.0. The pressure coefficient can be defined as

$$C_p = \frac{p}{\frac{1}{2}\rho u_{in}^2} \tag{5}$$

When r_2 is small, the recirculation zone cannot develop freely because most of the gas following impinging upon the glass plate flows out along the plate. Therefore, there is no region of negative pressure, and the injected gas stream pushes the plate without pulling it, as with existing designs of gas pads. It seemed difficult to obtain a levitation force when $r_2/H = 3.0$ because the region of negative pressure was too wide; the levitation force is only 13%, as compared to 0.03 Pa·m^2 when the ratio is 1.0.

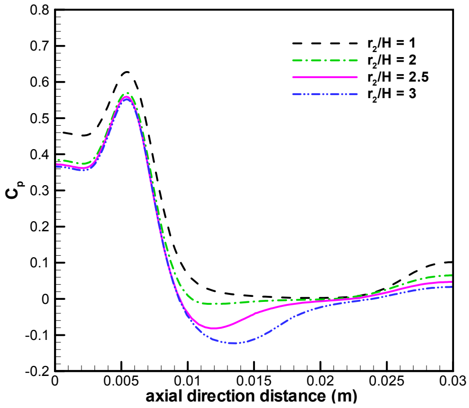

Fig. 5. Pressure coefficients for various values of r_2/H .

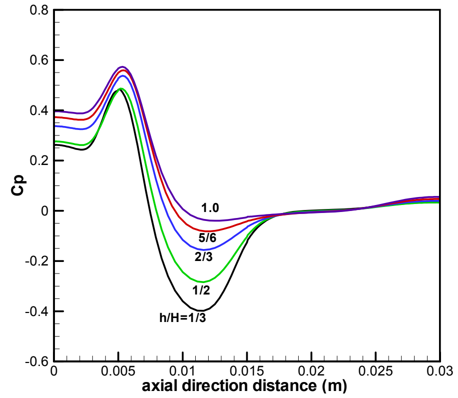

Fig. 6. Variation of the pressure coefficient with the normalized length, h/H , of the gap between the pad and the glass plate.

Fig. 6 shows the variation of the pressure coefficient with h , the distance between the gas pad and the glass plate. The speed of the gas flow increases as h decreases because a small value of h implies a narrow passage of flow. As a consequence of the Bernoulli theorem, the pressure coefficient becomes small as speed flow increases. It is possible to obtain both positive pressure for levitation and negative pressure for stability by adjusting the length of the gap between the glass plate and the pad. However, it is important to maintain the proper length of gap because a very narrow gap can cause damage to the glass plate when it vibrates or fluctuates during transportation.

4.2 Shape of effusion holes

Basically, high pressure can be obtained when a minimum amount of gas is effused. However, when

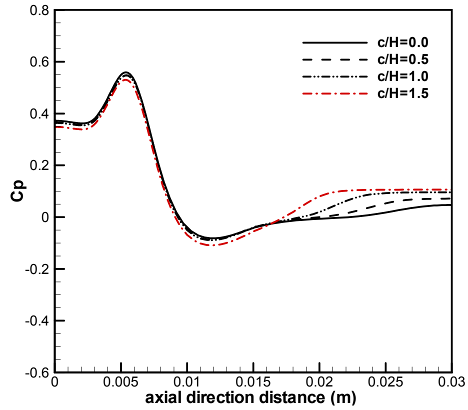

Fig. 7. Variation of the pressure coefficient with c/H.

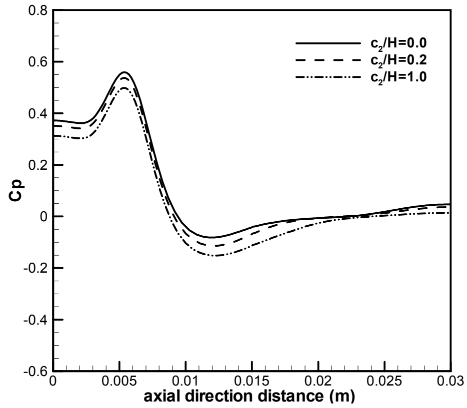

Fig. 8. Variation of the pressure coefficient with c_2/H.

stabilizing the glass plate, an appropriate amount of gas needs to flow out through the effusion holes [11]. Fig. 7 shows the variation of the pressure coefficient along the radial direction in relation to c . Up to an axial distance of 16 mm, c was seen to have little effect on the pressure around the injection nozzle. An increase in c produces a positive effect on the levitation force since pressure rises after 16 mm. The $c/H = 1.0$ was chosen instead of 1.5 due to the stability of the glass plate during transportation. The value should be adjusted in future experimental studies because stability analysis was not considered in this numerical study.

Fig. 8 shows the variation of the pressure coefficient with the parameter c_2 , which was clarified in Fig. 2. The overall pressure decreased slightly when c_2 was increased because a long and narrow passage of flow accelerates gas speed. It can be inferred that once a sufficiently negative pressure is obtained, an excessively large c_2 is unnecessary because of the resulting loss of the levitation force. We chose 0.0 because it provided the largest levitation force, and the profile of C_p was similar for the three values of c_2.

4.3 Heat transfer characteristics

The glass plate was coated by several materials, such as ITO and Cr, in the sputtering chamber. For efficient coating, the glass plate was heated up to 450 K. In general, a sputtering system has separate heating and process chambers for heating the glass plate prior to coating.

The glass plate was cooled down during transportation from chamber to chamber with the use of a gas jet. The characteristics of heat transfer are reported in this section. Based on the simulation results, $r_2/H = 2.5$, $h/H = 2/3$, $c/H = 1.0$, and $c_2 = 0.0$ were chosen as the optimal shape of the nozzle. The temperature of the glass plate was set to a uniform temperature of 413 K, which was the mean value of the temperature measured in the actual process [11].

Fig. 9 shows the Nusselt number profile on the glass surface as a function of the hydraulic diameter of the injection hole. The problem considered in this study was similar to the impinging-jet problem considered by Martin [12]. The Nusselt number profile showed a similar trend, as depicted by a dashed line, for the single-wall jet problem, which was considered by Martin [12]. Martin [12] also suggested the following equation for periodic, circular-jet arrays with period s and $Ar = \pi D^2/4s^2$.

$$\frac{\overline{Nu}}{\Pr^{0.42}} = 0.5K\left(Ar, \frac{H}{D}\right)G\left(Ar, \frac{H}{D}\right)\mathrm{Re}^{2/3} \tag{6}$$

In Eq. (6), K and G can be obtained from,

$$K = \left[1 + \left(\frac{H/D}{0.6/Ar^{1/2}}\right)^6\right]^{-0.05} \tag{7}$$

$$G = 2Ar^{1/2}\frac{1 - 2.2Ar^{1/2}}{1 + 0.2\left(H/D - 6\right)Ar^{1/2}}. \tag{8}$$

For the geometry shown in Fig. 2, the mean Nusselt numbers calculated from Eq. (6) using the hydraulic diameter, instead of D, were 23.1 and 23.5 for the gap-lengths of (H+h) and h, respectively. The simulated result, which was the average value of the local Nusselt number (Fig. 9), is 25.8, which is about 10% greater than those from Eq. (6). In light of the assumptions of adiabatic nozzles and constant glass temperature, the difference was not significant. It can be said that Martin's correlation on the nozzle array can be applied for the calculation of the cooling profile.

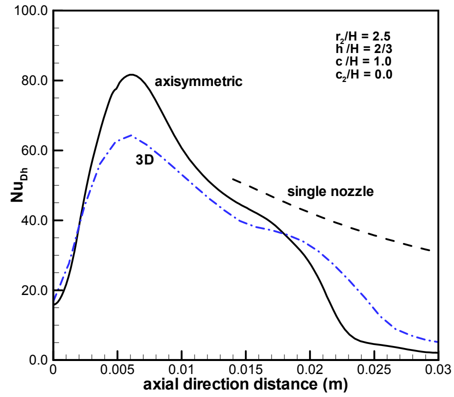

Fig. 9. Variation of the Nusselt number along the radial direction of the glass plate.

4.4 3-dimensional analysis

On the basis of the nozzle-shape that was determined in the previous sections, the configuration of the nozzle array was prepared for three-dimensional flow and heat transfer calculations. The boundary conditions were the same with the two-dimensional analysis except for the symmetric condition that was imposed at the cutting planes stem from the periodicity of the nozzle array.

Fig. 10 shows the velocity contours at the selected planes. After hitting the glass plate, gas flow change along the direction of the glass plate, and gas leaves the domain through effusion holes. Fig. 11 shows the pressure coefficient profile along the glass plate from the three-dimensional calculation along with the result from the optimal, two-dimensional, axisymmetric calculation. Results from the two-dimensional analysis are in good agreement with the result from the three-dimensional analysis although the two-dimensional domain was assumed to be axisymmetric. From this result, it appears that the two-dimensional axisymmetric approach of the previous section is valid.

The Nusselt number profile from three-dimensional analysis is plotted in Fig. 9. The average Nusselt number is 26.6, which is 3.1% greater than the result

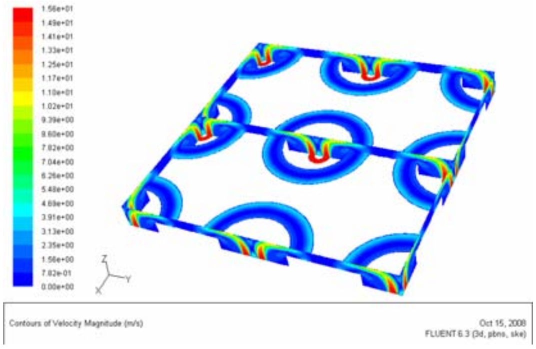

Fig. 10. Velocity contours at the selected planes from three-dimensional analysis.

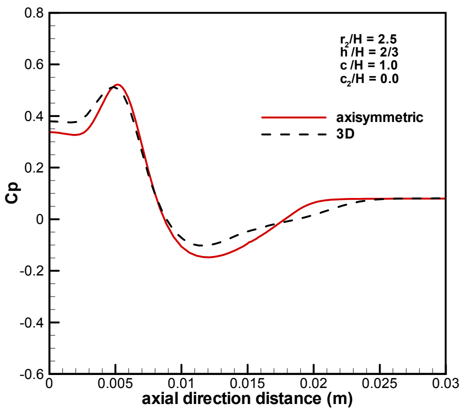

Fig. 11. Comparison of the pressure coefficient for two-dimensional and three-dimensional analysis.

from two-dimensional analysis, viz., 25.8. The drop in temperature of the glass plate during transportation can be predicted from the energy balance between the heat loss from the surface and the volumetric energy loss.

$$Q = hA(T_s - T_{gas}) = \rho V c_p \Delta T \tag{9}$$

where V is the volume of the glass plate. The heat transfer coefficient, h, which was calculated from the average Nusselt number, is 13.3 W/m^2-K. The predicted drop in the temperature of the glass plate is 1.1 K.

The k-ε turbulence model could be the reason why the Nusselt number is larger than Martin's correlation. The k-ε model overestimated the turbulent intensity at this flow-problem as compared to a relatively low Reynolds number. To clarify this point, the problem was re-analyzed using the k-ω turbulence model. The average Nusselt number resulting from the k-ω model is 22.7, while the drop in the temperature of the glass is 0.96 K. As expected, the k-ω model yields a Nusselt number that is 15% lower than in the k-ε model. However, it can be said that heat transfer is not an important concern because the temperature drop of about 1.0 K of the glass is negligible during the transportation.

5. Conclusions

In this study, the effects of the design variables of gas pads were numerically investigated for the non-contact transportation of glass plates in a sputtering system during the manufacture of LCD panels. To obtain information on the optimal design of pads, the variation of the pressure coefficients was plotted as a function of the dimensions of the shape of the nozzle.

In the case of small r_2 in relation to the recirculation zone, negative pressure for the stability of glass plates was not formed. As r_2 increased, the pressure decreased along with the loss of the levitation force. The region of negative pressure became large since either the length of the gap, *h*, between the pad and the glass plate or the levitation height decreased. Given that a very small gap causes damage to glass plates, the length of the gap has to be carefully determined. In terms of levitation force, the smallest region possible except the nozzle shoulder is desirable between the nozzles.

Furthermore, the Nusselt number profile of the glass plate resulting from the gas injection was considered in this study; it was similar to the convective heat transfer characteristics of wall jets. The average Nusselt number that was calculated from the k-ε model was 15% higher than in the k-ω model. It was also found that Martin's correlation, with regard to the circular nozzle array, was applicable for estimating rate of cooling.

Nomenclature

Ar : Area, shown in Eq. (6)
b : Width of a gas inlet (in Fig. 2)
C_p : Pressure coefficient
c : Length of the wall near the symmetric line (in Fig. 2)
c_2 : Length of the wall (in Fig. 2)
D : Diameter of a circular nozzle
H : Height of a bell-type nozzle (in Fig. 2)
h : Length of the gap between the gas pad and the

glass-plate
$\overline{Nu}$: Average Nusselt number
P : Mean static pressure
p : Instantaneous static pressure (Pa)
Pr : Prandtl number
R : Half of the distance between the injection holes
Re : Reynolds number
r_1, r_2 : Radii of the nozzle shown (in Fig. 2)
S_{ij} : Strain rate tensor
s : Period of the circular jet arrays
U_i : Mean velocity in tensor notation
u_i : Instantaneous velocity in tensor notation
u_i' : Fluctuating velocity in tensor notation
u_{in} : Velocity of the gas inlet (m/s)
V : Volume of the glass plate
x_i : Position vector in tensor notation

Greek symbols

ρ : density of the fluid
μ : dynamic viscosity of the fluid
τ_{ij} : Reynolds stress tensor, Eq. (3)

References

[1] F. Poh, T. Higuchi, K. Yoshida and K. Oka, Non-contact transportation system for thin glass plate utilizing combination of air bearing and electrostatic force, *SCIE'99*, 212 (B-2) (1999) 1053-1058.
[2] I.-T. Im, H. J. Jun and K. S. Kim, Numerical study on the air-cushion glass transportation unit for LCD panels, *J. of the Semiconductor and Display Equipment Tech.*, 5 (1) (2006) 27-31.
[3] T. Amano, Y. K. Nakamura, S. Ueha, Y. Hashimoto, A multi transducer near field acoustic levitation system for non-contact transportation of large-sized planar objects, *Jpn. J. Appl. Phys.* 39 (part I 5B) (2000) 2982-2985.
[4] I.-T. Im, H. J. Jeon, K. S. Kim and K.-W. Park, Optimization of the LCD panel air-cushion transportation unit using computational fluid dynamics, *The 2nd International Symposium on Micro and Nano Technology*, Hsinchu, Taiwan (2006).
[5] H. J. Jeon, K. S. Kim and I.-T. Im, Numerical study on the air-cushion unit for transportation of large-sized glass plate, *J. of the Semiconductor and Display Equipment Tech.*, 6 (1) (2007) 59-64.
[6] FLUENT is a product of Fluent Inc., 2003, 10 Cavendish Court, Centerra Resource Park, Lebanon, NH 03766, USA.
[7] W. P. Jones and B. E. Launder, The prediction of laminarization with a two-equation model of turbulence, *Int. J. of Heat Mass Transfer*, 15 (1972) 301-314.
[8] D. C. Wilcox, *Turbulence Modeling for CFD*, DCW Industries, Inc., La Canada, CA, U.S.A. (1993).
[9] FLUENT 6.1 User's Guide 2, 2003, Fluent Inc., Centerra Resource Park, 10 Cavendish Court, Lebanon, NH 03766, USA.
[10] P. Bradshaw, T. Cebeci and J. H. Whitelaw, Engineering *Calculation Methods for Turbulent Flow*, Academic Press, London (1984).
[11] AVACO Co., LG Phillips LCD Co., A Study on the development of the next generation sputtering equipment for LCD manufacturing, 1st Year Report, The Ministry of Commerce, Industry and Energy, Korea (2006).
[12] H. Martin, Heat and mass transfer between impinging gas jet and solid surfaces, in J. P. Hartnett and T. F. Irvine, Jr., (eds.), *Advances in Heat Transfer*, 13, Academic Press, New York (1977).

Ik-Tae Im received the B.S., M.S. and Ph.D. degrees in Mechanical Engineering from Hanyang Universsity, Seoul, Korea, in 1993, 1995 and 1999, respectively. He has been a visiting scientist at the Department of Materials Engineering, the University of Tokyo, Japan, from 2002 to 2003, where he have researched on the film growth during the MOCVD process. His research interests are the numerical modeling on the transport phenomena in various flow and heat transfer problems. He is an associate professor at the Department of Mechanical Design Engineering at Chonbuk National University, Korea.